C2012-0001683

Corrosion of Carbon Steel in High CO_2 Containing Environments - the Effect of High Flow Rate

A. Mohammed Nor, M. F. Suhor, M. F. Mohamed, M. Singer, and S. Nesic
Institute for Corrosion and Multiphase Flow,
Ohio University, Athens, OH 45701

ABSTRACT

The development of hydrocarbon gas fields which contain very high CO_2 contents (up to 80 mol%) using carbon steel seems a difficult proposal and calls for the use of expensive corrosion resistant alloys. This would have the potential to render project development costs untenable. Unlike transportation and sequestration of supercritical CO_2, where the amount of water is normally very small or negligible, gas field development has to consider the presence of formation water. This water can contain a high concentration of corrosive species, generated by large amounts of dissolved CO_2. The magnitude of corrosion and the effect of flow on corrosion in such environments are unknown and a better understanding is required. Flow has the possible effects of challenging the protectiveness of any corrosion product films that may form and will increase the mass transfer rates of corrosive species to the pipe wall, both leading to an increase in corrosion rate.

In the present study, a High Pressure and High Temperature (HPHT) Thin Channel Flow Cell (TCFC) was employed to study the flow sensitivity of CO_2 corrosion of carbon steel, at subcritical and supercritical CO_2 partial pressures. The corrosion rate measured in the TCFC was related with the one obtained in a HPHT rotating cylinder electrode (RCE) autoclave tests. This was done to ascertain the independence of the measured corrosion rates from the specific flow geometry.

Keywords: *Supercritical CO_2, rotating cylinder electrode, flow-sensitive corrosion, thin-channel flow cell, equivalent velocity.*

INTRODUCTION

South East Asia has about 182 Tcfg undeveloped hydrocarbon gas reserves. One of the reasons that these reserves have not been fully harnessed is that they reside in high CO_2 containing fields; for example, Natuna D-Alpha field in Indonesia contains about 70 mole percent of CO_2.[1] At the outset, the development of these fields would call for the use of expensive corrosion resistant alloys due to the possibility of high CO_2 corrosion of carbon steel. This would potentially render the project development costs untenable. An alternative approach would be to evaluate the technical feasibility of using carbon steel. Unlike transportation and sequestration of supercritical CO_2, where the amount of water is normally negligible or comes from condensation,[2] field development has to consider the presence of formation water which has the potential of containing a high concentration of corrosive species due to dissolved CO_2. For offshore installation, it would be too costly to dry the gas stream or to remove the CO_2 gas prior to transportation of hydrocarbon gas via pipelines. While the presence

of water and dissolved CO_2 may render the environment very corrosive to carbon steel, it is suspected that the flow of the corrosive liquid over the metal surface could possibly enhance the corrosion rate even further. This is because flow increases the mass transfer rates of the corrosive species to the pipe wall and challenges the integrity and protectiveness of the corrosion product films.[3,4]

In an earlier study carried out using an autoclave and a high pressure high temperature rotating cylinder electrode (HPHT RCE) autoclave system, the results suggested a low flow-sensitivity of CO_2 corrosion at a high partial pressure of CO_2 .[5] However, that study was limited to a liquid velocity of 1 m/s. In the current study, a different flow geometry was used – channel flow (also called: flow between two parallel plates). The liquid velocity in this high pressure high temperature thin channel flow cell (HPHT TCFC) was varied from 0 m/s to 8 m/s.

In order to compare and connect the corrosion rate results from the two flow systems, all the operational parameters and water chemistry must be the same, and the velocity needs to be adjusted so that the mass transfer conditions are the same, in accordance with Silverman and Nesic.[6-8]

For the RCE, one can use the Eisenberg's mass transfer correlation,[9] given by equation (1) below:

$$Sh_c = 0.0791\left(Re_c{}^{0.7}\right)\left(Sc^{0.356}\right) \quad (1)$$

where:

$Sh_c = \frac{k_c d_c}{D}$ – is the Sherwood number for the RCE ;
k_c – is the mass transfer coefficient for the RCE in $\left(\frac{m}{s}\right)$;
d_c – is the diameter of the cylindrical specimen in (m) ;
D – is the diffusion coefficient in $\left(\frac{m^2}{s}\right)$;
$Re_c = \frac{V_c d_c}{\nu}$ – is the Reynolds number for the RCE ;
V_c – is the peripheral velocity of the cylindrical specimen in $\left(\frac{m}{s}\right)$;
ν – is the kinematic viscosity of water in $\left(\frac{m^2}{s}\right)$;
$Sc = \frac{\nu}{D}$ - is the Schmidt number.

For the TCFC, one can use the Sleicher and Rouse mass transfer correlation,[10] given by equation (3) below:

$$Sh_T = 5 + 0.015\left(Re_T{}^{a}\right)\left(Sc^{b}\right) \quad (2)$$

where:

$Sh_T = \frac{k_T h}{D}$ – is the Sherwood number for the the TCFC ;
k_T – is the mass transfer coefficient for the TCFC in $\left(\frac{m}{s}\right)$;
h – is the height of the TCFC ;
$Re_T = \frac{V_T h}{\nu}$ – is the Reynolds number for the TCFC ;
V_T - is the linear velocity of the liquid in the TCFC in $\left(\frac{m}{s}\right)$;
a, b – are empirical constants defined by:

$$a = 0.88 - \frac{0.24}{(4 + Sc)} \quad (3)$$

$$b = \frac{1}{3} + 0.5e^{(-0.6Sc)} \quad (4)$$

Equating the mass transfer coefficients k_c and k_T for the two flow geometries enables us to calculate the equivalent flow velocity in the TCFC which results in the same mass transfer coefficient seen in the RCE and the same corrosion rate. An example of the equivalent velocities for the two flow systems used in the present study are given in Table **1** below.

Table 1

The equivalent velocities for RCE and TCFC used in the experiments.

	RCE Peripheral Velocity / (m/s)	TCFC Linear Velocity / (m/s)
1	0	0
2	0.5	0.8
3	1.0	1.5
4	-	8

EXPERIMENTAL

It must be noted that the focus in this study was on single-phase turbulent flow. Corrosion rates were measured in the TCFC using weight loss and electrochemical methods at various temperatures (25 - 80°C), CO_2 partial pressures (10 - 80 bar), and liquid velocities (0 - 8.0 m/s). The pH of the aqueous solution was autogenous (governed by dissolved CO_2) and did not change significantly during the experiments.

Test Specimen

In the experiment, the two key methods for determining the CO_2 corrosion rate were linear polarization resistance (LPR) measurements and the weight loss (WL) methods. Figure 1 shows the LPR probe and the WL specimen used in this work. The three-electrode LPR probe was used to follow the time evolution of the corrosion rate. It consisted of three concentric steel elements electrically separated by epoxy: the center element and the outer ring were made out of UNS S31600 stainless steel while the middle ring was made of API[(1)] 5L X-65 carbon steel machined from a retrieved line pipe. The center element served as a reference electrode while the outer ring served as the counter electrode. The total exposed surface area of the carbon steel ring was 0.95 cm^2.

The weight loss (WL) specimen was used for measuring the time-averaged CO_2 corrosion rate and for cross-validation with LPR measurements. The back and the sides of the WL specimen were double coated with Xylan[(2)] paint, so as to ensure no electrical contact between the specimen and the specimen holder. The chemical composition of the carbon steel and the surface preparation of the specimens prior to exposure to test solution were described in an earlier paper.

Test Equipment and Instrumentation

The experiments were conducted in a 70-L High Pressure and High Temperature (HPHT) Thin Channel Flow Cell (TCFC) system. The main element of this system is the test section in the form of a rectangular cross section flow channel, shown in Figure 2. The dimensions of the flow channel are: height: 3 mm, width: 100 mm, and

(1) American Petroleum Institute, 1220 L Street, NW Washington, DC 20005-4070
(2) Trade name

length: 740 mm. This flow geometry ensured fully developed, well characterized turbulent flow at the locations where the corrosion probes were flush mounted.

The full HPHT TCFC system is shown in Figure 3 below. It enabled saturation of the aqueous solution with high pressure CO_2 and full control of temperature, pressure, flow rate, and water chemistry. The water and CO_2 were equilibrated in the pressure vessel and then only the CO_2 saturated water was pumped toward the test section. To measure the pH of the test solution, a high pressure and high temperature glass pH probe and Ag/AgCl reference electrode probe were inserted into the pressure vessel. A potentiostat/galvanostat was employed for electrochemical measurements (LPR). A spectrophotometer was used to occasionally measure the concentration of ferrous ions in the aqueous solution (iron counts) and these measurements were then converted into a corrosion rate and compared to WL and LPR measurements.

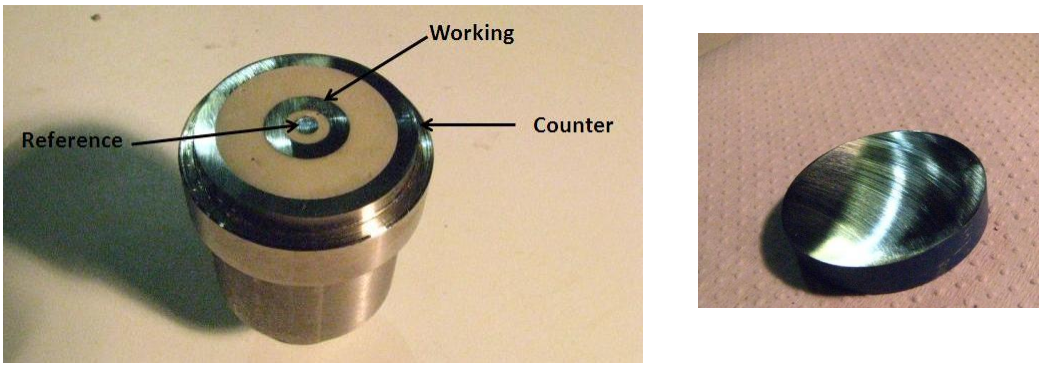

Figure 1: The three-electrode LPR probe and the WL specimen used in the HPHT TCFC.

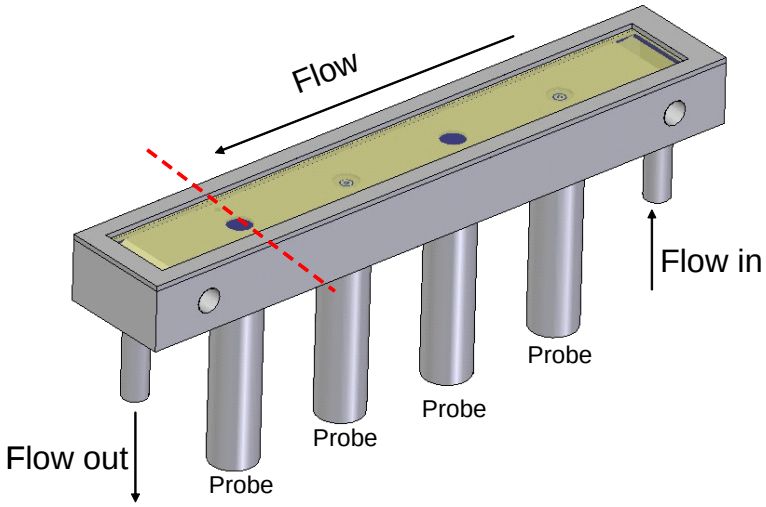

Figure 2: A drawing of the flow channel test section which is the main part of the HPHT TCFC, showing the four positions where corrosion probes/specimen were inserted.

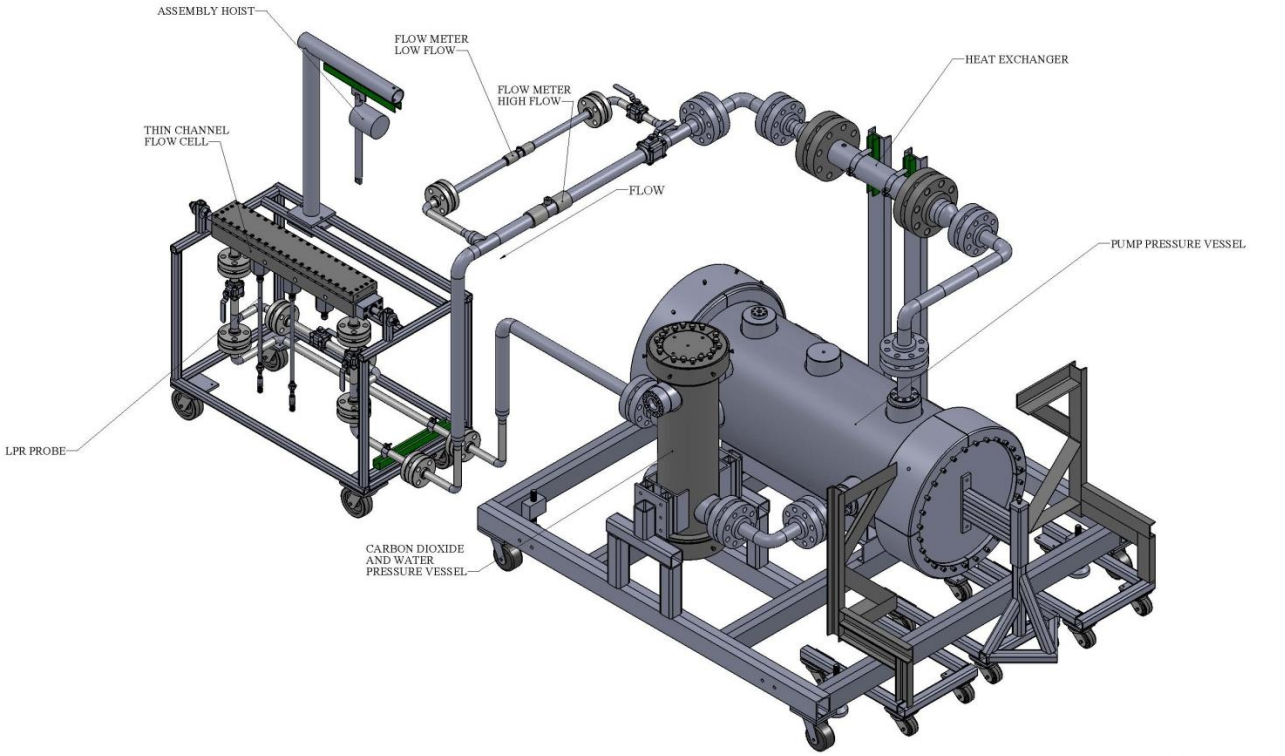

Figure 3: A drawing of the HPHT TCFC system showing the main components.

Test Procedure

The LPR and WL specimens mounted on their respective holders were inserted flush-mounted inside the flow channel test section. After that, the test section was pressurized to the desired pressure using nitrogen gas and isolated from the rest of the TCFC system by closing the inlet and outlet valves. This was done to protect the test specimen from corrosion while bringing the whole TCFC system to the desired pressure and temperature and to prevent a sudden pressure surge when test solution was introduced into the test section.

Sixty liters of 1 wt. % NaCl aqueous solution was pumped into the pressure vessel. The test solution was de-aerated using a CO_2 purge until the concentration of dissolved oxygen reached undetectable levels (typically less than 5 ppb) as determined by colorimetric measurements. The test solution was then heated to the desired test temperature. At the test temperature, the vessel was then gradually pressurized to the required CO_2 partial pressure. The pH of the test solution was followed and the actual corrosion measurements were not started before the solution reached the autogeneous pH (shown in Table 2) as calculated by a custom built water chemistry model.[11] This was to ensure that the test solution was fully saturated with dissolved CO_2, a process which took a long time (6 – 48 h) depending on the other conditions. Finally, when the solution was deemed ready, it was pumped through the flow channel test section and the corrosion measurements were initiated.

Table 2
The key experimental conditions: CO_2 partial pressure and state, temperature and the water pH

CO_2 Partial Pressure (bar)	Temperature	
	25 °C	80 °C
10	Gaseous CO_2, water pH 3.4	
80	Liquid CO_2, water pH 3.0	Supercritical CO_2 , water pH 3.2

Prior to taking the LPR measurements, the open-circuit potential of the specimen was measured until it became relatively stable (within ±1 mV). LPR measurements were carried out twice at each velocity which was varied from stagnant to 8 m/s and back to stagnant. In the LPR tests, the specimen was polarized ±5 mV from the open-circuit potential at a scan rate of 0.125 mV/s. The polarization resistance was compensated for the effect of solution resistance which was determined by using high frequency EIS measurements (100 kHz). The full EIS spectra were recorded at the end of the test and will be reported in a separate publication.

Weight loss test was also carried out using an exposure period of 24 hours or less. The purpose was to validate the results from the electrochemical experiments. At the end of the experiment, test solution was sampled and analyzed using spectrophotometer for iron counts.

RESULTS

The corrosion rate measurements obtained by LPR are show in Figure 4, Figure 5 and Figure 6. The results generated in the RCE are compared with those from the TCFC at various equivalent liquid velocities as outlined in Table 1. The calculation of corrosion rate from polarization resistance measurements used 26 mV as the Stern-Geary coefficient (**B** value).[12] The use of this **B** value assumes that the corrosion rate was under limiting current control. In addition, it was shown in this and some previous similar work that this **B** value yielded LPR corrosion rate which overall correlated best with corrosion rates obtained from weight loss and iron counts.

The first fact that needs to be noted is that at these high CO_2 concentrations, all the measured corrosion rates were very high, and in some cases extreme (at 80°C). The results also suggest that at 25°C, the corrosion rate did not change considerably with liquid velocity, even at pCO_2 of 80 bars. This was confirmed by measurements taken in both the RCE and the TCFC, which agreed rather well – within the margin of experimental error. The finding confirms the assumption that using these two very different flow geometries would yield a similar corrosion rate when all the experimental conditions are equivalent – including the mass transfer rate. The absence of flow dependence for the corrosion rate at 25°C is likely due to the dominant effect of carbonic acid reduction which is limited by the hydration of dissolved CO_2. [13]

On the other hand, when the temperature was increased to 80°C, the corrosion rates of RCE and TCFC differed significantly (Figure 6**)**. The TCFC corrosion rate was one order of magnitude higher than that of RCE, and it showed a significant flow-sensitivity. The large difference in the corrosion rates obtained using the two flow geometries is discussed below.

In Figure 7 and Figure 8 below, the surface images and elemental analysis for the low-temperature test conditions (25 °C) are shown, indicating that the corrosion product layers consisted mainly of non-protective cementite (Fe_3C), which represents the uncorroded portion of the steel. At high temperature (80°C) and high pCO_2 (80 bars), some ferrous carbonate ($FeCO_3$) crystals are seen, mixed in with the cementite, which was confirmed by X-ray diffraction (XRD) analysis. In all cases, a severely corroded steel surface was revealed after the corrosion product layer was removed, without any indications of localized attack.

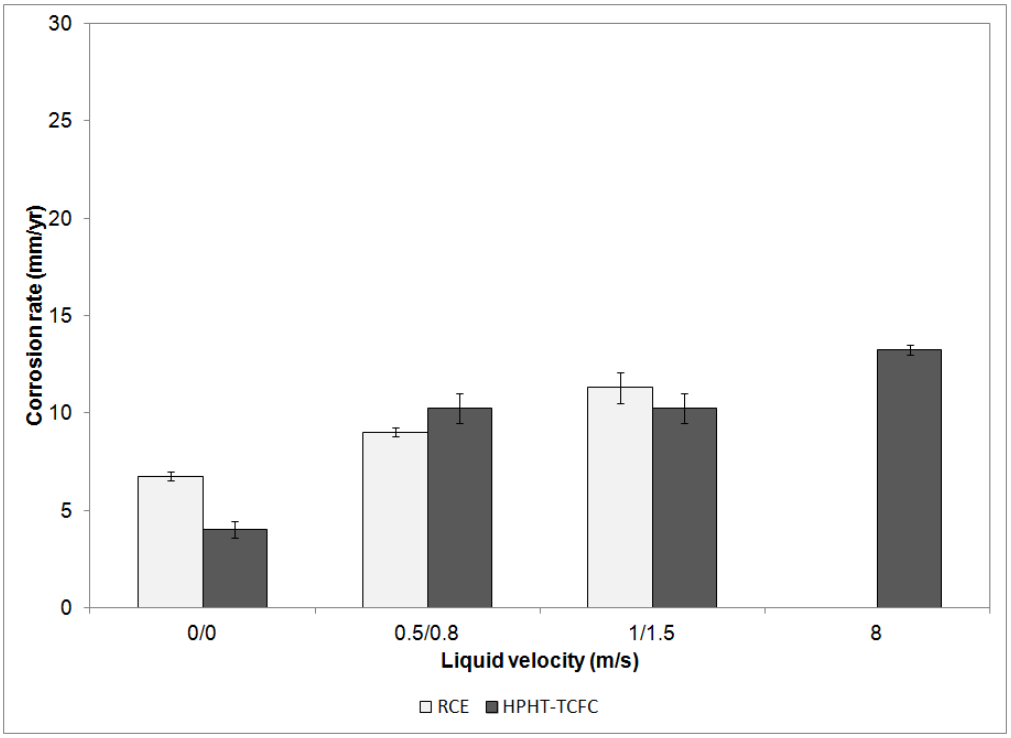

Figure 4: The corrosion rate obtained by LPR as a function of liquid velocity at pCO_2 of 10bar, 25 ^{o}C, and pH 3.4 . Data from a Rotating Cylinder Electrode (RCE) are compared to those from a Thin Channel Flow Cell (TCFC) for the equivalent velocity.

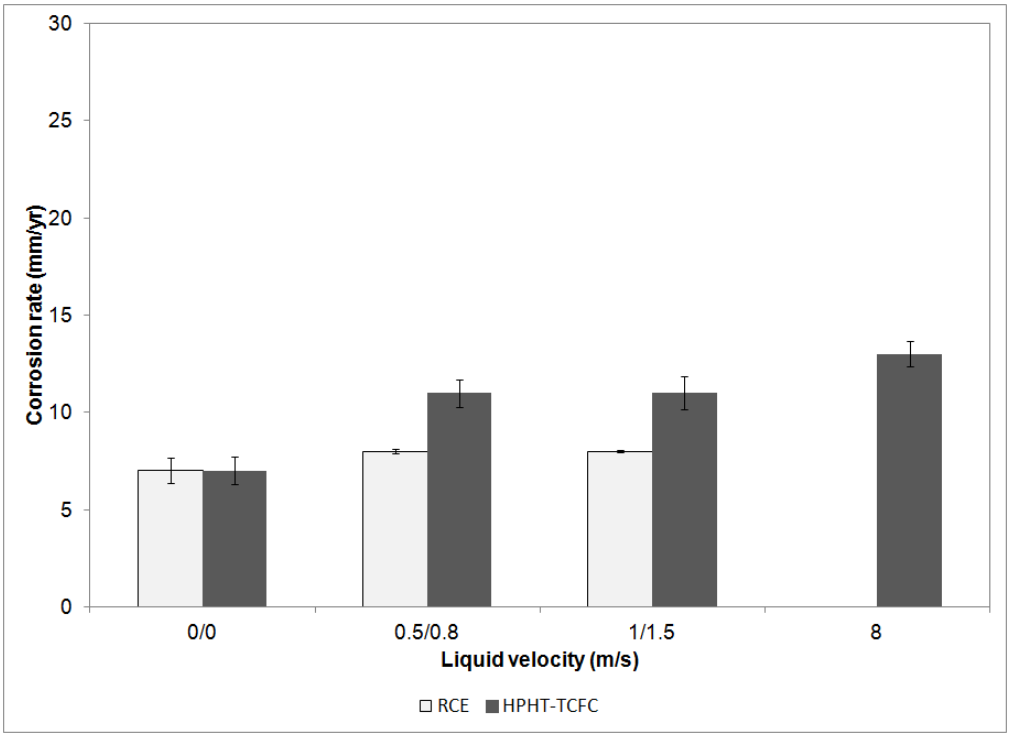

Figure 5: The corrosion rate obtained by LPR as a function of liquid velocity at at pCO_2 of 80bar, 25 ^{o}C, and pH 3. Data from a Rotating Cylinder Electrode (RCE) are compared to those from a Thin Channel Flow Cell (TCFC) for the equivalent velocity.

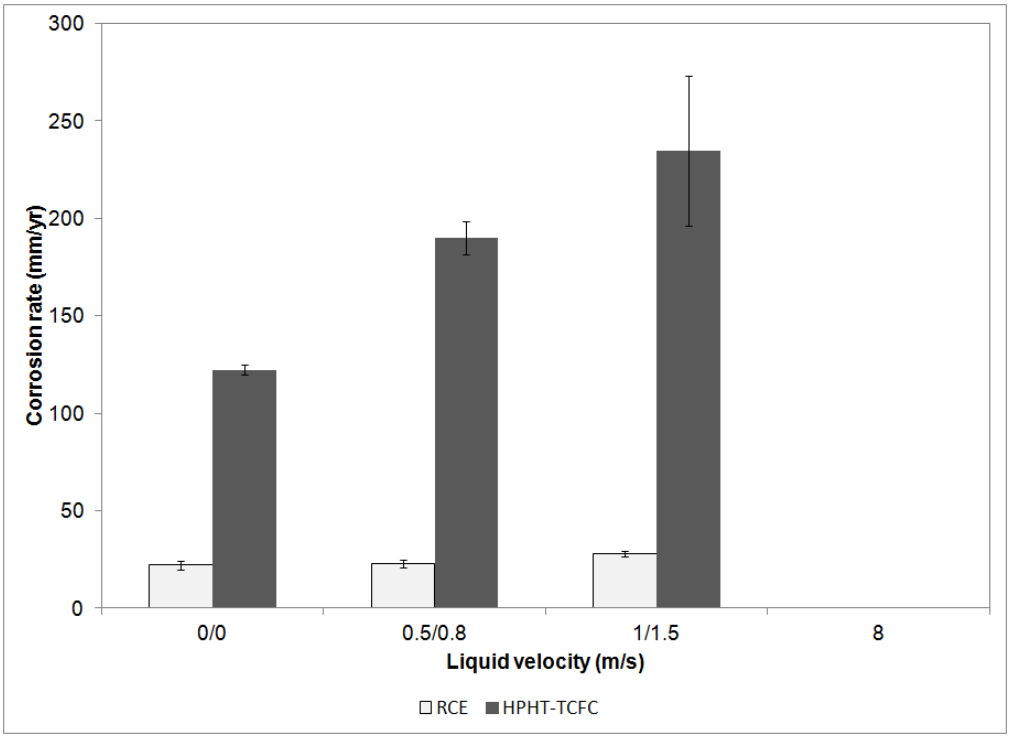

Figure 6: The corrosion rate obtained by LPR as a function of liquid velocity at at pCO_2 of 80bar, 80 ^{o}C, and pH 3.2. Data from a Rotating Cylinder Electrode (RCE) are compared to those from a Thin Channel Flow Cell (TCFC) for the equivalent velocity.

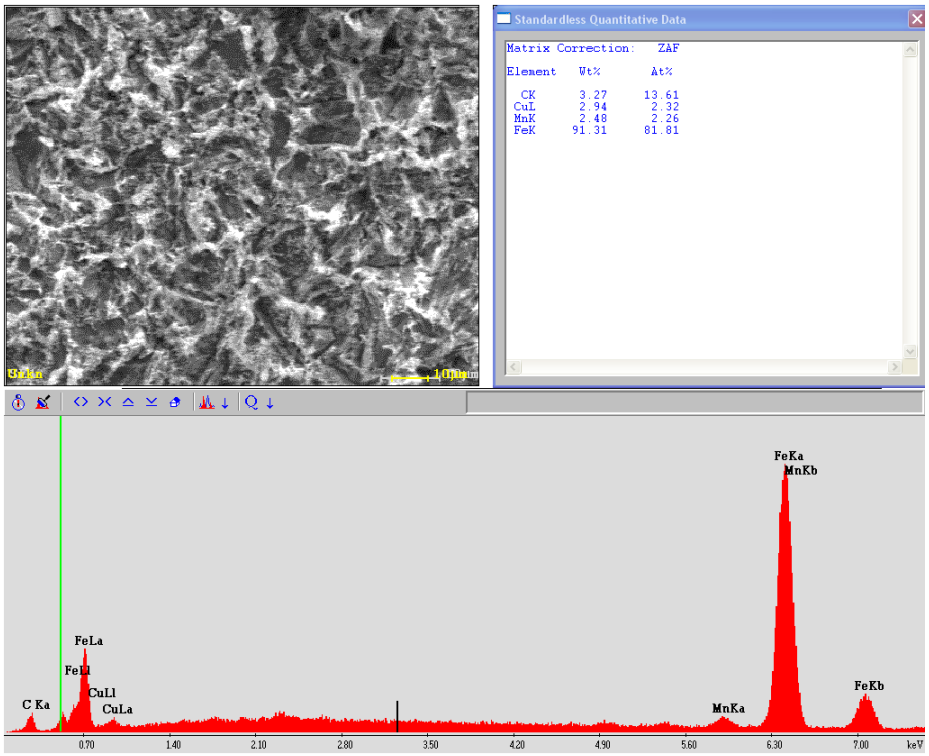

Figure 7: A surface image and elemental analysis of the corrosion product layer obtained using EDX, suggesting the presence of cementite (iron carbide) with some minor alloying elements; steel sample exposed to water saturated with pCO_2=10bar, at 25^{o}C, and pH 3.4 for 24 h.

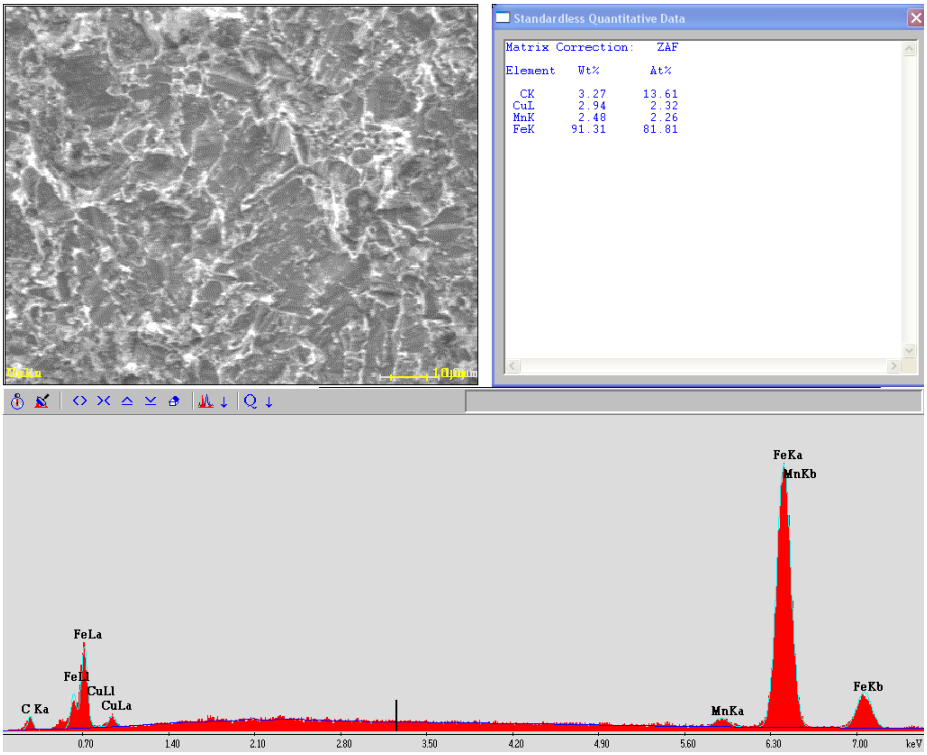

Figure 8: A surface image and elemental analysis of the corrosion product layer obtained using EDX, suggesting the presence of cementite (iron carbide) with some minor alloying elements; steel sample exposed to water saturated with pCO_2=80bar, at 25°C, and pH 3 for 24 h.

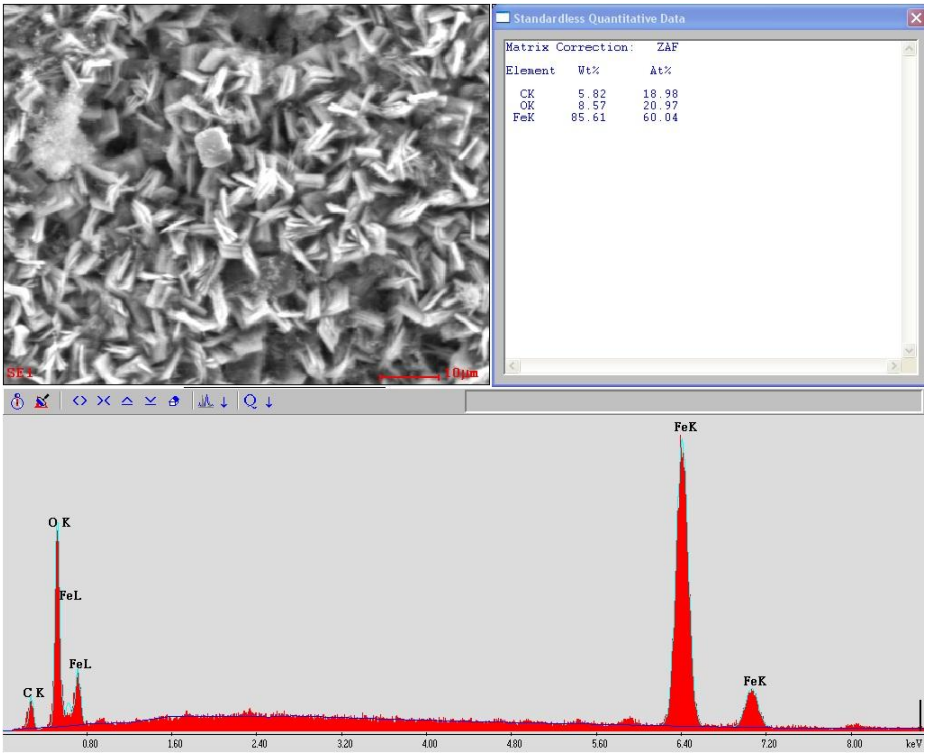

Figure 9: A surface image and elemental analysis of the corrosion product layer obtained using EDX, suggesting the presence of cementite (iron carbide) and siderite (iron carbonate); steel sample exposed to water saturated with pCO_2=80bar, at 80°C, and pH 3.2 for 24 h.

The differences in corrosion rates between the RCE and the TCFC seen in Figure 6 have most likely arisen from the differences in water chemistry evolving throughout the experiment. This could be deduced from the measured

pH values of the test solution and the iron counts. It was observed that at 80°C the measured pH in the TCFC test solution did not change significantly in the course of the experiment. In comparison, the measured pH of the RCE test solution increased from 3.2 to 3.6 over the same time period, due to the higher concentration of ferrous ions (iron counts) released by corrosion. At the end of the experiment, the RCE test solution contained a ferrous iron concentration of about 330 ppm while the TCFC solution only had 13 ppm. The reason for this is the difference in the volume of the test solution: for the RCE experiments it was only 5 liters while for the TCFC it was 70 liters. Consequently, a high concentration of ferrous ions and the higher pH of RCE test solution could have facilitated the formation of a somewhat protective ferrous carbonate layer, leading to lower corrosion rates.[14, 15] This difference between the two systems was only pronounced at 80 °C, when the initial corrosion rates were much higher – releasing more corrosion products into the solution and when the formation of iron carbonate was kinetically favorable.[19, 20] It is considered that the corrosion rates obtained in the TCFC were more realistic.

CONCLUSIONS

1. The corrosion rates of carbon steel obtained at high partial pressures of CO_2 (10–80 bar) were very high.
2. Given the correct choice of equivalent velocities, the corrosion rates obtained in the RCE autoclave and the TCFC correlated well at low temperature (25°C), indicating a flow geometry-independent corrosion rate.
3. The TCFC with its larger volume of test solution produced more realistic corrosion rates, particularly at a higher pCO_2 (80 bar) and higher temperature (80°C) as one could avoid a large build up of corrosion products and an unrealistic change in water chemistry in the TCFC.
4. The increase in temperature seems to have increased the flow-sensitivity of CO_2 corrosion of carbon steel.

ACKNOWLEDGEMENTS

The authors would like to extend their deep appreciation and gratitude to PETRONAS for its financial support, Dr Sa'adan Mat for initiating and supporting this project, Mr. Steven Upton, whose dedication ensured the TCFC experiments could be completed successfully, and Mr. Albert Schubert, Mr. Bruce Brown, Mr. Cory Shafer, and Mr. Daniel Cain, who sacrificed their time and comfort and went out of their way to ensure the experiments were executed safely and timely.

REFERENCES

[1] J. Veron, "An overview of the non-developed gas reserves in southeast Asia," *PetroMin, (3),* pp. 22-28, 2007.

[2] M. Seiersten and K. O. Kongshaug,"Materials selection for capture, compression, transport and injection of CO_2," in *Carbon Dioxide Capture for Storage in Deep Geologic Formations - Results from the CO_2 Capture Project Capture and Separation of Carbon Dioxide from Combustion Sources,* Amsterdam: Elsevier, 2005, pp. 937.

[3] A. Dugstad, L. Lunde and K. Videm, "Parametric study of CO_2 corrosion of carbon steel," in *CORROSION/94,* paper no. 14 (Houston, TX: NACE, 1994).

[4] T. Y. Chen, A. Moccari and D. D. MacDonald, "The development of controlled hydrodynamic techniques for corrosion testing," *Corrosion,* vol. 48, *(3),* pp. 239-255, 1992.

[5] A. Mohammed Nor, M. F. Suhor, M. F. Mohamed, M. Singer and S. Nesic, "Corrosion of Carbon Steel in High CO_2 Environment: Flow Effect," CORROSION/*2011,* paper no. 11245 (Houston, TX: NACE, 2011).

[6] D. C. Silverman, "Technical note: On estimating conditions for simulating velocity-sensitive corrosion in the rotating cylinder electrode," *Corrosion,* vol. 55, *(12),* pp. 1115-1118, 1999.

[7] D. C. Silverman, "Technical note: Conditions for similarity of mass-transfer coefficients and fluid shear stresses between the rotating cylinder electrode and pipe," *Corrosion,* vol. 61, *(6),* pp. 515-518, 2005.

[8] S. Nesic, G. T. Solvi and J. Enerhaug, "Comparison of the rotating cylinder and pipe flow tests for flow sensitive CO_2 corrosion," *Corrosion,* vol. 51, *(10),* pp. 773-787, 1995.

[9] M. Eisenberg, C. W. Tobias and C. R. Wilke, "Ionic mass transfer and concentration polarization at rotating electrodes," *Electrochemical Society -- Journal,* vol. 101, *(6),* pp. 306-320, 1954.

[10] C. A. Sleicher and M. W. Rouse, "Convenient correlation for heat transfer to constant and variable property fluids in turbulent pipe flow," *Int. J. Heat Mass Transfer,* vol. 18, *(5),* pp. 677-683, 1975.

[11] M. F. Mohamed, A. Mohammed Nor, M. F. Suhor, M. Singer, Y. S. Choi and S. Nesic, "Water Chemistry for Corrosion Prediction in High-pressure CO_2 Environments," CORROSION */2011, p*aper no. 11375 (Houston, TX: NACE, 2011).

[12] S. Papavinasam, "Electrochemical techniques for measuring corrosion rates in operating oil and gas pipelines," in *NACE 2010/097X,* 2010, Technical Information Exchange.

[13] S. Wang, K. George and S. Nesic, "High pressure CO_2 corrosion electrochemistry and the effect of acetic acid," CORROSION */2004,* paper no. 04375 (New Orleans, LA: NACE 2004).

[14] S. Nesic and K. J. Lee, "A mechanistic model for carbon dioxide corrosion of mild steel in the presence of protective iron carbonate films - part 3: Film growth model," *Corrosion,* vol. 59, *(7),* pp. 616-628, 2003.

[15] W. Sun, S. Nešić and R. C. Woollam, "The effect of temperature and ionic strength on iron carbonate (FeCO3) solubility limit," *Corros. Sci.,* vol. 51, *(6),* pp. 1273-1276, 2009.

[16] M. Seiersten, "Material Selection for Separation, Transportation and Disposal of CO_2," in CORROSION */2001, p*aper no. 01042 (Houston, TX: NACE, 2001).

[17] M. F. Suhor, M. F. Mohamed, A. Mohammed Nor, M. Singer and S. Nesic, "Corrosion tests of mild steel in high pressure CO2 environments," *NACE Research in Progress, NACE Research in Progress* 2011. Corrosion/2011 (Houston, TX: NACE, 2011).

[18] K. Videm and A. Dugstad, "Corrosion of carbon steel in an aqueous carbon dioxide environment. part 1: Solution effects," *Mater. Perform.,* vol. 28, *(3),* pp. 63-67, 1989.

[19] C. de Waard, U. Lotz and D. E. Milliams, "Predictive model for CO_2 corrosion engineering in wet natural gas pipelines," *Corrosion,* vol. 47, *(12),* pp. 976-985, 1991.

[20] A. Dugstad, "Mechanism of Protective Film Formation during CO_2 Corrosion of Carbon Steel," CORROSION */98,* paper no. 31 (San Diego, CA: NACE, 1998), P. 31/1.

[21] E. Eriksrud and T. Sontvedt, "Effect of flow on CO_2 Corrosion Rates in Real and Synthetic Formation waters," CORROSION */83,* paper no. 44 (Houston, TX: NACE, 1983), p. 20.